NASA Technical Memorandum 110336

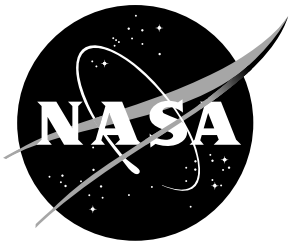

Vertical Tail Buffeting Alleviation Using Piezoelectric Actuators - Some Results of the Actively Controlled Response of Buffet-Affected Tails (ACROBAT) Program

Robert W. Moses
Langley Research Center, Hampton, Virginia

April 1997

National Aeronautics and
Space Administration
Langley Research Center
Hampton, Virginia 23681-0001

Vertical Tail Buffeting Alleviation Using Piezoelectric Actuators - Some Results of the Actively Controlled Response of Buffet-Affected Tails (ACROBAT) Program

Robert W. Moses
Aeroelasticity Branch
NASA Langley Research Center
Hampton, VA

Abstract

Buffeting is an aeroelastic phenomenon associated with high performance aircraft especially those with twin vertical tails. In particular, for the F/A-18 aircraft at high angles of attack, vortices emanating from wing/fuselage leading edge extensions burst, immersing the vertical tails in their wake. The resulting buffet loads on the vertical tails are a concern from fatigue and inspection points of view. A 1/6-scale F-18 wind-tunnel model was tested in the Transonic Dynamics Tunnel at the NASA Langley Research Center as part of the Actively Controlled Response Of Buffet Affected Tails (ACROBAT) program to assess the use of active controls in reducing vertical tail buffeting. The starboard vertical tail was equipped with an active rudder and the port vertical tail was equipped with piezoelectric actuators. The tunnel conditions were atmospheric air at a dynamic pressure of 14 psf. By using single-input-single-output control laws at gains well below the physical limits of the actuators, the power spectral density of the root strains at the frequency of the first bending mode of the vertical tail was reduced by as much as 60 percent up to angles of attack of 37 degrees. Root mean square (RMS) values of root strain were reduced by as much as 19 percent. Shown herein, a single-input-single-output may be employed at constant gain throughout the angle of attack range without requiring adaptations. Future tests are mentioned for accentuating the international interest in this area of research.

Keywords: piezoelectric, buffeting alleviation, active controls

Nomenclature

α, AOA	angle of attack, degrees	q, Q	dynamic pressure
c, *c*, $\bar{c}$	characteristic length (mean chord)	$\ddot{x}$, $\ddot{y}$	acceleration
f, *f*	frequency, Hz	m(t), M(f)	unmeasured input noise to system
f_b	frequency of first bending mode	x(t), X(f)	measured input to system
t, T	time	y(t), Y(f)	measured output of system
U, V	air speed	H(f), H_{xy}(f)	system transfer function
δ	control surface deflection	S, G	autospectral functions
ϕ, θ	phase angle, radians	n	Strouhal frequency parameter

Subscripts

b	first bending mode	x	input
y	output		

1.0 Introduction

Buffeting is an aeroelastic phenomenon which plagues high performance aircraft especially those with twin vertical tails. As shown in figure 1, for aircraft of this type at high angles of attack, vortices emanating from wing/fuselage leading edge extensions (LEX) burst, immersing the vertical tails in their wake. The resulting buffet loads on the vertical tails are a concern from fatigue and inspection points of view [1-4]. For example, for the McDonnell-Douglas F/A-18, special and costly 200-flight-hour inspections are required to check for structural damage due to buffet loads [4]. Inspections and repairs are high cost items to the military services.

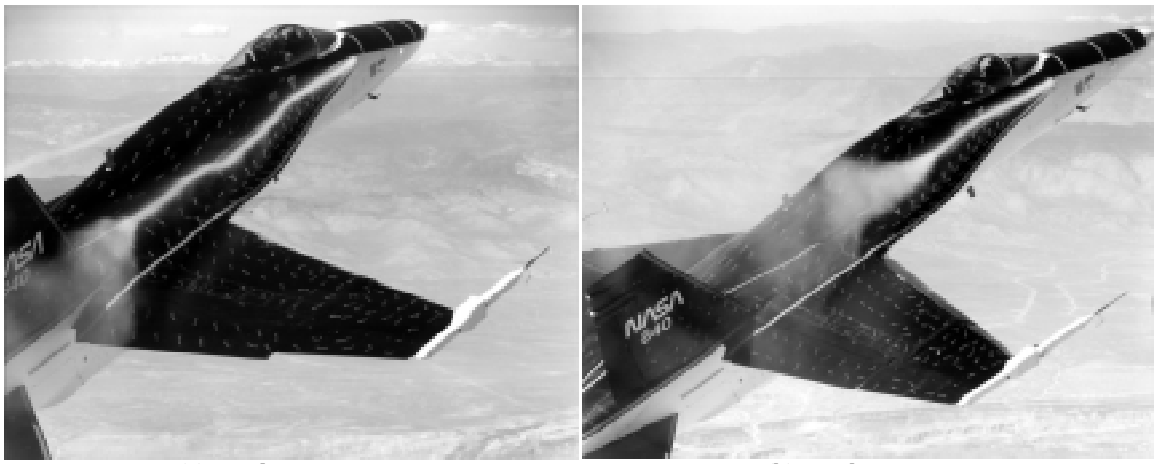

(a) 20 degrees AOA (b) 30 degrees AOA

Figure 1. Flow Visualization of Leading Edge Extension (LEX) Vortex Burst

As shown in figure 1, the LEX vortex bursts ahead of the tail around 20 degrees angle of attack. This burst point moves further ahead of the tail with increased angle of attack. To illustrate the flow field just ahead of the tail at high angles of attack, flow visualizations are presented for angles of attack between 15 and 35 degrees in a vertical-lateral plane passing through the leading-edge root of the tail, as shown in figure 2. At 20 degrees, the core of the vortex is still intact, as seen in figure 2(b). However, at 30 degrees, the core has broken down completely in the plane ahead of the tail, and the entire vertical tail is engulfed in the turbulence.

To reduce fatigue and thus increase the life of a vertical tail, the stress values must be reduced. This reduction may be accomplished by 1) either modifying the load-carrying structure within the tail, 2) reducing the buffet loads by altering the flowfield around the vertical tail, or 3) by reducing the buffeting response by adding damping. The success of a proposed fix to the buffet problem has generally been measured by percentage reduction in the root mean square (rms) of the strain at the root of the vertical tail.

For the purpose of understanding the buffeting problem, several programs focused on quantifying the buffet loads by acquiring response measurements and surface pressures on the vertical tails of scaled models in a wind-tunnel and on an actual aircraft during flight[1-3, 5-13]. In general, the results of these studies are published as spectra and pressure coefficients for the inboard and outboard surface of the tail.

Based on some of these studies, McDonnell-Douglas Aircraft (MDA) implemented an interim solution on the F-18 relying entirely upon structural modifications to the vertical tail in an attempt to reduce the dynamic stresses in critical areas[2]. Even with the structural enhancement, the dynamic stresses were still too severe. This led to the investigation of a LEX configuration that was found to reduce the dynamic loading of the vertical tail[2]. After numerous engineering studies, wind-tunnel tests, and flight tests by MDA, the US Navy adopted the LEX fence as a retrofit for its fleet of F-18 aircraft. Based on a wind-tunnel test of a 6% F-18 model, the LEX fence was found to: 1) reduce the unsteady lift and pitching moment of the aircraft, 2) increase the unsteady pressure fluctuations on the upper surface of the LEX, and 3) reduce the steady and unsteady pressures on the vertical tail. During flight tests, where data is acquired during a range of transient dynamic pressure and transient angle of attack, called q-band and a-band, respectively, the LEX fence reduced the peak accelerations in the first two modes of the vertical tail. Although the loads on the vertical tail were found to be reduced by the LEX fence, there have been some concerns of the impact on aircraft performance stemming from items one and two mentioned above. The desired approach to resolving the vertical tail buffeting problem is to maintain, if not enhance, overall aircraft performance, while reducing the dynamic stresses in the critical areas of the aircraft. From this standpoint, other options needed to be explored.

In 1992, the concept of an actively controlled rudder was extended to alleviating vertical tail buffeting[14]. To approximate the rudder output and the generalized aerodynamic forces around the vertical tail, a doublet-lattice method was used with a reduced value of dynamic pressure. The corresponding aerodynamic damping and stiffness were combined with the structural model to derive an open-loop, state-space realization of the F-18 vertical tail at 32 degrees

angle-of-attack, which is considered the worst case. Using this semi-empirical effectiveness of the rudder, this analysis of an actively controlled rudder showed that damping could be added to the tail resulting in reductions in the strain at the root of the tail.

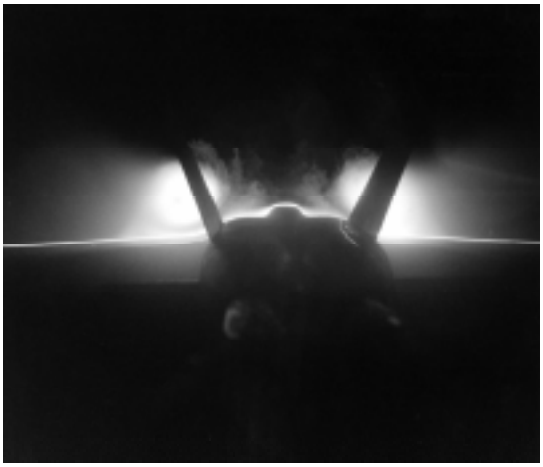

(a) α = 15 degrees

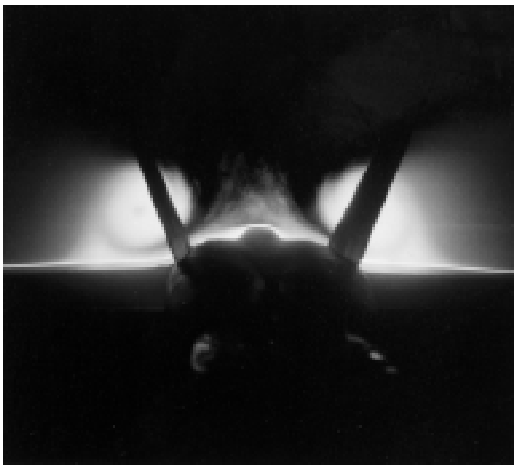

(b) α = 20 degrees

(c) α = 25 degrees

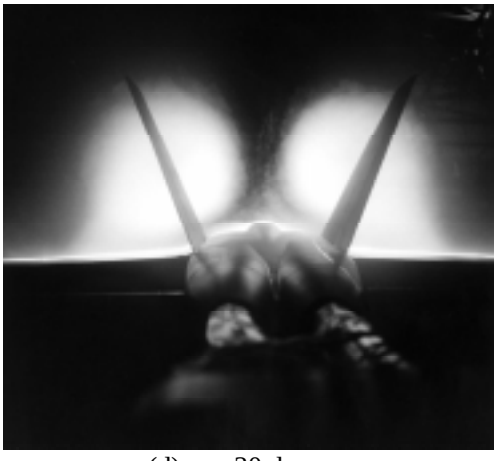

(d) α = 30 degrees

(e) α = 35 degrees

Figure 2. Vortex Characteristics at Vertical Tail Leading Edge
For Five Angles of Attack

In 1995, the use of actively controlled piezoelectric actuators on an F/A-18 vertical tail was analyzed[15]. Incorporating approximations of the unsteady aerodynamics, this analysis showed that actively controlled piezoelectric actuators could increase damping greater than 60% in the first bending mode for less than an 8% increase in the weight of the vertical tail.

In 1995, vertical tail buffeting alleviation was achieved using piezoelectric actuators on a 5%-scale 76-/40-deg double delta wing wind-tunnel model with twin vertical tails that were not canted[16]. This 15-inch-long fuselage was constructed from a flat plate and resembled an F-15 planform. The 4.5-inch tall vertical tails, one rigid and one flexible, were symmetric about a vertical axis, resembling isosceles triangles that had been cropped at the top. Over ranges of angle of attack from 20 to 55 degrees and dynamic pressure from 0.5 to 7 psf, peak response of the vertical tail was reduced by as much as 65% over the uncontolled response, using simple control algorithms employing collocated strain gauges.

In 1995, a wind-tunnel investigation at the Transonic Dynamics Tunnel (TDT) at the NASA Langley Research Center (LaRC) extended the promising analysis of active buffeting alleviation to an experimental demonstration[17]. The research objectives of the ACROBAT program at LaRC are twofold: 1) to determine the spatial relationships of the differential pressures during open-loop and closed-loop conditions at various angles of attack; and, 2) to apply active controls technology, using a variety of force producers, to perform buffet load alleviation on twin vertical tails of a 1/6-scale F-18 wind-tunnel model. This investigation is the first experimental demonstration of active buffeting alleviation on a scaled F-18 wind-tunnel model using an active rudder and piezoelectric actuators.

The main purpose of this paper is to present some open-loop and closed-loop results for the ACROBAT program's wind-tunnel tests of active piezoelectric actuators used to alleviate vertical tail buffeting. Results when using the actively controlled rudder are provided for comparison. Without the uncertainties from using analytical tools to model the aerodynamics, the results of the wind-tunnel tests, presented herein, demonstrate the feasibility of using actively controlled piezoelectric actuators (as well as a rudder) to alleviate vertical tail buffeting on an F-18 configuration. Stability gain margins are presented for illustrating active control system stability at the angles of attack tested.

2.0 Wind-Tunnel Model

An existing 1/6-scale, rigid, full-span model of the F/A-18 A/B aircraft was refurbished, and three flexible and two rigid vertical tails were fabricated. This model was then sting-mounted in the Transonic Dynamics Tunnel (TDT) at the NASA Langley Research Center, as shown in figure 3, where it underwent a series of tests to determine buffet flowfield characteristics and alleviate vertical tail buffeting.

The three flexible tails were fabricated from a 1/8-inch thick aluminum plate and covered with balsa wood. The aluminum plate thickness was chosen such that the frequencies of the first three modes were close to those of the actual tail as determined by a finite element analysis. Also, by using a frequency scaling near unity, the effects of actuator bandwidth could be compared directly between full-scale and reduced-scale results. All three flexible tails were instrumented with a root strain gage aligned to measure bending moment and with two tip accelerometers near the leading and trailing edges. For the port tail, positive root strains occur for tail motions outboard while positive tip accelerations occur for tail motion inboard. Positive commands to the piezoelectric actuators at the root of the port vertical tail moved the tip of the port vertical tail inboard. The two rigid tails (one port, one starboard) were fabricated from a block of aluminum and were geometrically identical to the flexible tails.

To investigate the active alleviation of vertical tail buffeting, the flexible tails included the following actuators: 1) a rudder surface; 2) a tip vane configuration containing a slotted cylinder; 3) piezoelectric actuation devices; or 4) an embedded slotted cylinder. The rudder, the tip vane, (shown in figure 4) and the embedded slotted cylinder were activated by clamping each of them (when necessary) to a drive shaft that was turned by a hydraulic actuator located below the root of the vertical tail. Each of the seven opposing pairs of piezoelectric actuators, shown in figure 5(b), were powered by individual amplifiers located outside the test section of the TDT. For the port flexible tail with active piezoelectric actuators, the first bending mode is around 14 Hz (wind-off) and the first torsion mode is around 62 Hz (wind-off). Not counting bonding material, each piezoelectric actuator at the root of the vertical tail consisted of two stacks of four layers of encapsulated wafers. The actuators at other span locations consisted of two stacks of two layers of encapsulated wafers. Each actuator at the root had dimensions of 4.00"x1.50"x0.06" and weighed 1.02 ounces (2.1% of total vertical tail

weight). Each actuator at other span locations had dimensions of 4.00”x1.50”x0.03” and weighed 0.51 ounces. There are a total of six actuators at the root and eight actuators elsewhere.

Figure 3. 1/6-Scale F/A-18 Model Mounted in the Transonic Dynamics Tunnel

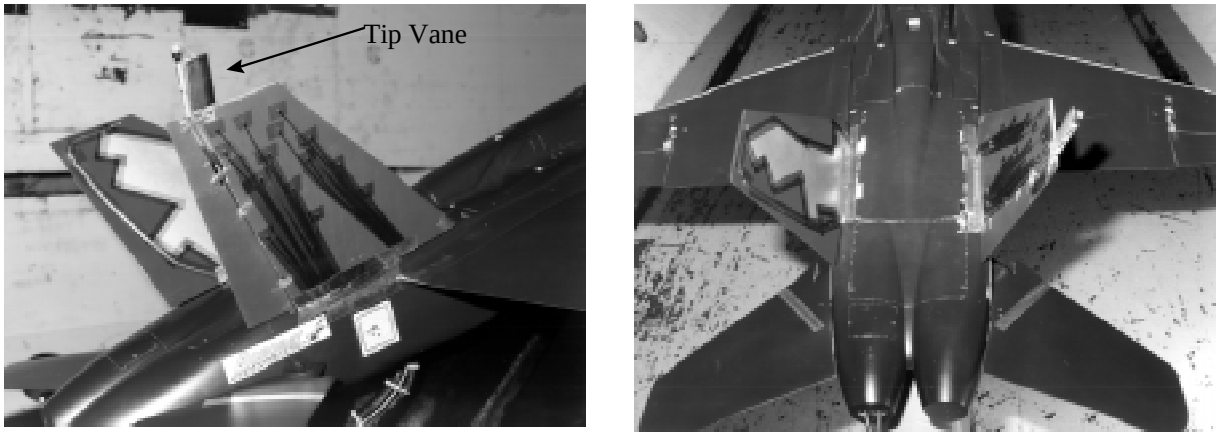

(a) Side View (b) Top View

Figure 4: Views of 1/6-Scale F/A-18 Model Mounted in the TDT

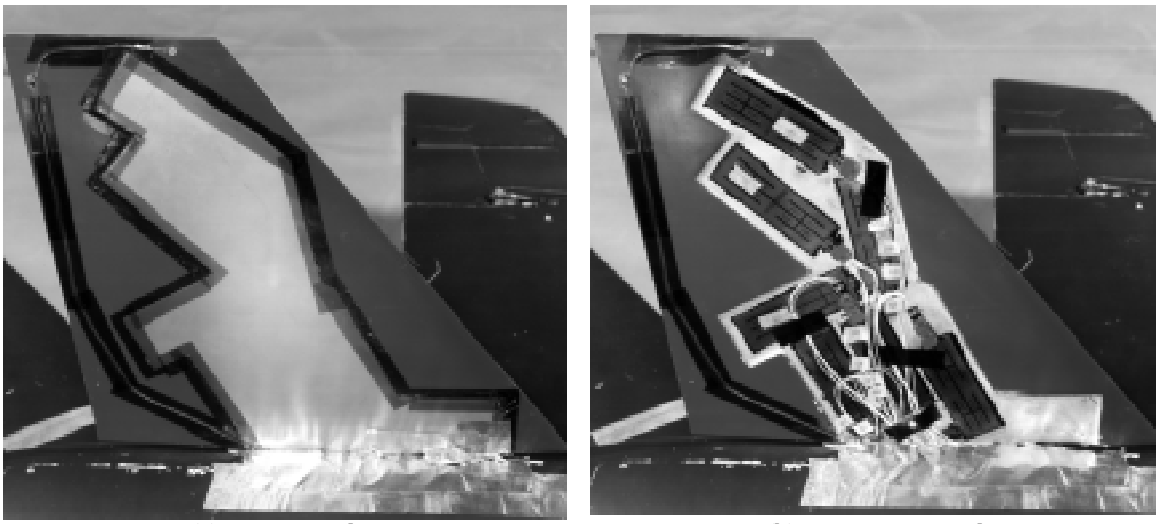

(a) Cover In Place (b) Cover Removed

Figure 5. Piezoelectric Actuator Arrangement on Port Flexible Tail

3.0 Test Conditions

For buffet, the Strouhal number is the primary scaling relationship used in determining tunnel conditions[1]. The Strouhal number, *n*, is a nondimensional frequency parameter that is proportional to reduced frequency, and is expressed as

$$n = \frac{f \cdot c}{U}$$

where *f* is frequency in Hz, *c* is characteristic length, and *U* is velocity.

Since active controls were a primary focus, comparisons of actuator bandwidths between model and flight were an issue. Therefore, to avoid any difficulties in scaling and defending any possible discrepancies, a frequency ratio between model and aircraft structural modes and forcing function spectra of unity was chosen, leaving only two variables, *c* and *U*, to be determined. According to the Strouhal number, to match frequency content between aircraft models of different scales, the relationship of c divided by U must be identical. Since 1/6-scale model was chosen, only one variable, *U*, needed to be determined. According to reference 1, the dynamic pressure where vertical tail buffeting appeared maximum was roughly 340 psf. Using a value for air density at an altitude of approximately 12,000 feet, velocity was determined. For the case of a 1/6-scale wind-tunnel model that has a frequency ratio of one with the aircraft, the windspeed requirement is 1/6 of the flight speed of the aircraft. For the ACROBAT program, a tunnel speed of 110 feet per second (14 psf) was used.

4.0 Data Acquisition, Processing, and Control Systems

The response data was recorded by an active system and a passive system. The active system, consisted of a SUN 3/160 Workstation driven by a UNIX operating system[18]. This system was capable of acquiring time history records for 32 channels at frequencies up to 200 Hz for lengths up to 150 seconds. The passive system was capable of sampling 64 channels at rates up to 500 Hz and was used to verify the data collected by the active digital controller. The data collected on the passive system was also used to determine time delays associated with the active digital controller.

A second SUN Workstation, configured similarly to the active system, was used not only as a backup to the active system, but also as a near real-time multisignal digital analyzer for estimating both the open- and closed-loop plants and computing stability margins to evaluate control law performance[19]. Time-domain functions and frequency-domain functions were computed from the time histories using the Signal Processing Toolbox in Matlab. Matlab was later installed on an additional computer, a Silicon Graphics Challenge L, for assisting in the nearly real-time data processing.

The active system, consisted of a SUN 3/160 Workstation driven by a UNIX operating system[18]. This SUN also served as the active digital controller (ADC) which generated the actuator commands based on loaded control laws. This system had three special purpose processing units linked via a data BUS, which included an integer digital signal processor (DSP), a floating point DSP board with two microprocessors, and an array processor (AP). The ADC chassis housed the host CPU, the disk and tape drives, and the added boards that all communicated across a VME data BUS. The host CPU and the status display panel provided user interface to the real-time system. A SKY Computers, Inc. Challenger-1 (C1) integer DSP board controlled the real-time processing. Most control law computations were performed on a SKY Challenger-C30/V (C30). This was a high-speed, floating point, 32-bit systems-oriented digital signal two-processor board. The AP was another SKY board that provided high-speed direct memory access for the ADC and vectorized floating point processing. Two analog-to-digital (A/D) and two digital-to-analog (D/A) converter boards, manufactured by Data Translation, Inc., provided the link between the digital controller and the analog hardware, providing all the analog/digital data conversions required between the model and the ADC. They converted the incoming analog voltages from the sensors to 12-bit digital values and 12-bit digital signals such as the control surface actuator commands into outgoing analog voltages. The entire real-time operation from sensor input to actuator command output was repeated at regulated speeds up to a maximum requirement of 200 times each second. A filter box housed analog antialiasing filters, analog notch filters, and electrical isolation networks. The analog antialiasing filters were configured to provide either first-order rolloff or fourth-order rolloff with either a 25- or 100-Hz break frequency. The sensor signals coming to the ADC or the commands going to the model could be filtered through analog notch filters, if desired, to filter out undesired frequency ranges.

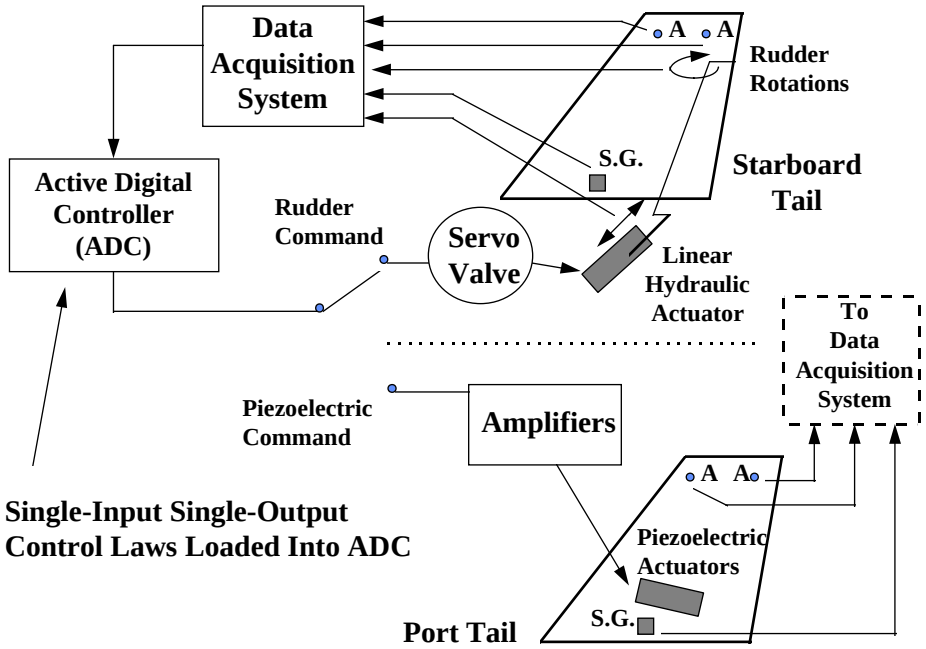

Figure 6. Active Control System

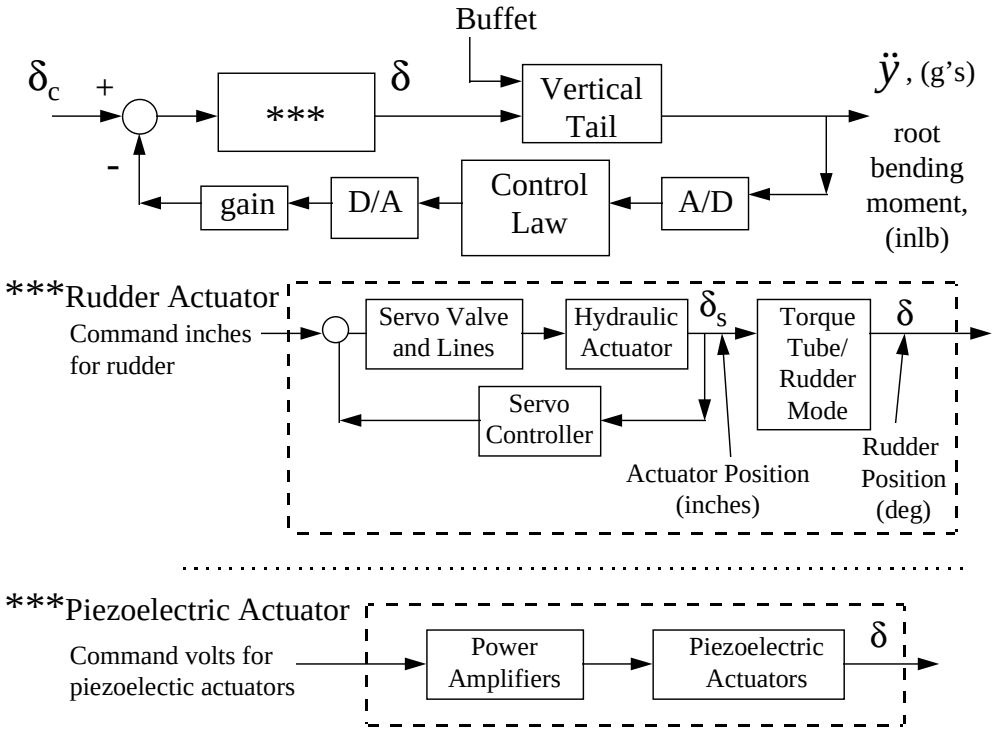

Figure 7. Block Diagram of Active Control System

The hardware of the active digital controller, as shown in figure 6, consists of the wind-tunnel model components and the active (computer) system described above. The digital controller, called the active digital controller in figure 6, was

modified to suit the needs of the present program. By converting to block diagram form, as shown in figure 7, the forward and feedback loops can be illustrated. The forward loop consists of the actuator and the remaining components of the vertical tail. For instance, the "actuator" for the starboard tail consists of the rudder, its hydraulic actuator, and the servo valve and its controller. The "vertical tail" for the starboard side consists of the tail components minus the rudder.

5.0 General Buffet and Buffeting Characteristics of the Wind-Tunnel Model

Typically, the buffet and buffeting are quantified by their dimensional or nondimensional power spectral density (PSD) functions. Since the results reported for this test are not being compared to other model or aircraft data, the dimensional form is used. In depth studies on buffet pressure characteristics and vertical tail buffeting have been performed on full-scale and model-scale F-18 vertical tails [1-3, 5-13].

For the1/6-scale F-18 model, the power spectral density plots of the unsteady differential pressures of the buffet at angles of attack of 20, 26, and 34 degrees are shown in figure 8. Since there were no pressure transducers located on the port tail, the differential pressures were computed from the pressure time histories acquired near the center of the planform of the starboard flexible tail. The buffet at 20 degrees AOA, in figure 8(a), appears broad band compared to the buffet at 26 degrees AOA, in figure 8(b). At 26 degrees AOA, an aerodynamic resonance around 40 Hz has emerged. At 34 degrees AOA, the magnitude of the aerodynamic resonance has grown while its location has shifted to a lower frequency (near the frequency of the first bending mode of the tail). These trends of the pressures with angle of attack are consistent with other experimental data[1, 8].

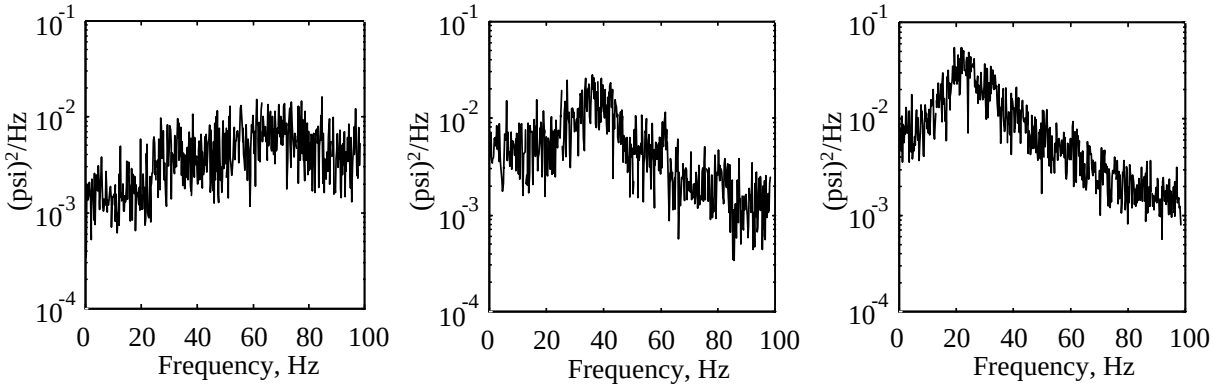

(a) 20 Degrees AOA (b) 26 Degrees AOA (c) 34 Degrees AOA

Figure 8. PSDs of Differential Buffet Pressure, Midspan Midchord, Starboard Flexible Tail at 3 Angles of Attack, 14 psf

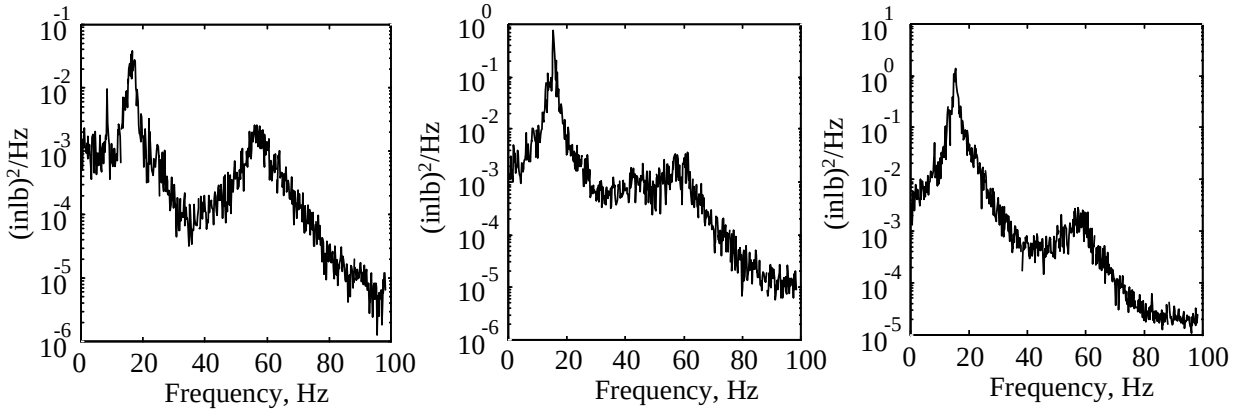

(a) 20 Degrees AOA (b) 26 Degrees AOA (c) 34 Degrees AOA

Figure 9. PSDs of Root Bending Moment Buffeting Response, Starboard Flexible Tail at Three Angles of Attack, 14 psf

The pressures, shown in figure 8 (a)-(c), created the buffeting, or structural response to the buffet, shown in figure 9 (a)-(c), respectively. At 34 degrees angle of attack, the buffeting shown in figure 9(c) around 14 Hz, which corresponds to the first bending mode of the vertical tail, has intensified by 1.5 and 0.5 orders of magnitude above the level at 20 degrees AOA, shown in figure 9(a), and the level at 26 degrees AOA, shown in figure 9(b), respectively. Since the buffet, or force input to the tail, has shifted to a lower frequency with increased angle of attack, as indicated by figure 8, the resulting vertical tail buffeting mainly consists of a response in the first bending mode, as indicated by comparing figures 9 (a) and 9 (c). The response in the mode around 58 Hz has not grown significantly with the increase in angle of attack because the magnitude of the pressures in that portion of the spectrum has not increased with increased angle of attack, as seen in figure 8. Referred to as "open-loop" buffeting, the structural responses due to the buffet only (without a commanded signal to the rudder or piezoelectric actuators) peaked at an angle of attack of approximately 34 degrees for the 1/6-scale F-18 model. This peak at 34 degrees angle of attack agrees well with the results of other wind-tunnel tests[1, 8].

Another influence of the buffet on the vertical tail buffeting was seen by comparing the first bending frequency of the vertical tail as angle of attack was changed. The frequency of the first bending mode shifts to a lower value as angle of attack is increased, as summarized in figure 10. This gradual shift in frequency with angle of attack can also be seen in the results of another wind-tunnel test that examined vertical tail buffeting on a 12% F-18 full-span model[1]. If the vertical tail is considered a single degree-of-freedom system subject to the large perturbations in the flow due to the burst vortex, then this shift in frequency may be viewed as increases in aerodynamic damping of the first bending mode. During the current ground vibration test of the starboard flexible tail, the structural damping was computed as approximately 1.8 percent for the wind-off damped first bending mode. Using the relationship between damped frequency and natural undamped frequency, the undamped natural frequency of the tail was calculated and used in estimating the total damping from the damped natural frequencies observed in the wind-tunnel at each angle of attack. The aerodynamic damping was calculated simply by subtracting the structural damping from the total damping. As seen in table 1, the aerodynamic damping reaches approximately 7 percent at 37 degrees angle of attack.

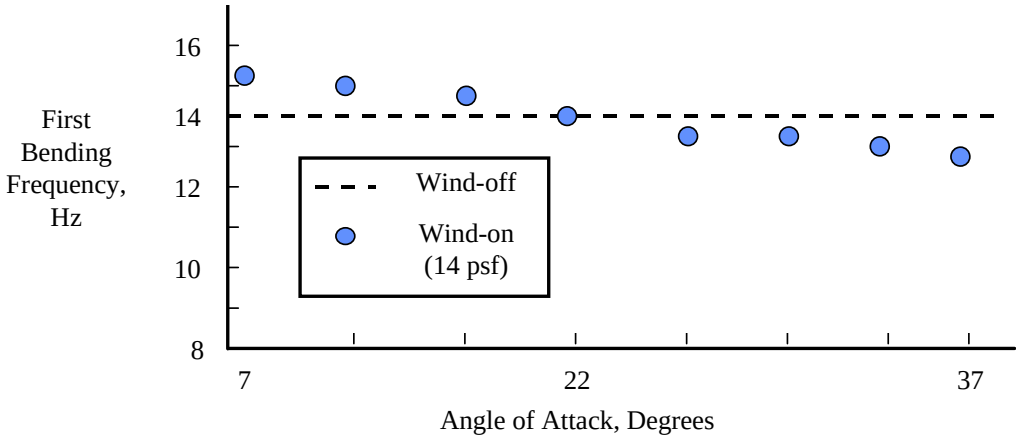

Figure 10. Variations of First Bending Frequency vs. Angle of Attack

Table 1. Estimates of Aerodynamic Damping Associated With Measured Vertical Tail First Bending Mode

Angle of Attack, deg	Aerodynamic Damping, percent
26	4.2
30	4.2
34	5.6
37	7.0

Referred to as "open-loop" buffeting, the structural responses due to the buffet only (without a commanded signal to the rudder or piezoelectric actuators) peaked at an angle of attack of approximately 34 degrees for the 1/6-scale F-18 model. This peak at 34 degrees angle of attack agrees well with the results of other wind-tunnel tests[1, 8]. The power spectral density (PSD) and root mean square (RMS) quantities of tip acceleration and root bending moment are normalized to their maximum values and presented in table 2 for the port tail. The PSD values shown are the magnitudes at the frequency of the first bending mode, f_b .

Table 2. Open-Loop Tip Acceleration and Root Bending Moment of Port Tail, Normalized to Maximum Open-Loop Value

Angle of Attack, deg	PSD(f_b) of tip acceleration	RMS(total acceleration signal)	PSD(f_b) of root bending moment	RMS(total root bending moment signal)
28	.3	.74	.29	.58
30	.36	.81	.35	.67
32	.68	.9	.65	.8
34	1	.98	.94	.93
35	.95	1	1	1
37	.7	.94	.74	.94

6.0 System Identification of the Wind-Tunnel Model Leading to Active Vertical Tail Buffeting Alleviation

The open-loop frequency response functions of the vertical tails due to the piezoelectric actuators were acquired experimentally by performing fast fourier transforms[20] on the time histories of the responses of the commanded actuators and sensors located on the vertical tails. On-line capabilities at the TDT allowed quick computations of frequency response functions from time histories acquired just minutes earlier. No analytical predictions of the frequency response functions were made in advance of the wind-tunnel test because no analytical models of the aerodynamics associated with buffet were available at that time. The open-loop frequency response functions reported herein were obtained at a dynamic pressure of 14 psf in atmospheric air.

Several commands were sent separately to each actuator for determining the open-loop frequency response functions. To concentrate on the first bending mode around 15 Hz, a maximum frequency of 20 Hz was generally used in a linear frequency sweep. At times, linear sweeps up to 40 Hz were used to determine the influences of modes at frequencies higher than the frequency of the first bending mode of the vertical tail. In some cases, periodic pseudonoise (PPN) was used since this signal randomly selects the frequency content rather than sweeping through a mode which could result in damage to the wind-tunnel model. A matrix of transfer functions was obtained for all piezoelectric actuator pairs (as input) and the following outputs: strain at the root of the vertical tail, tip accelerations near the leading edge of the vertical tail, and tip accelerations near the trailing edge of the vertical tail.

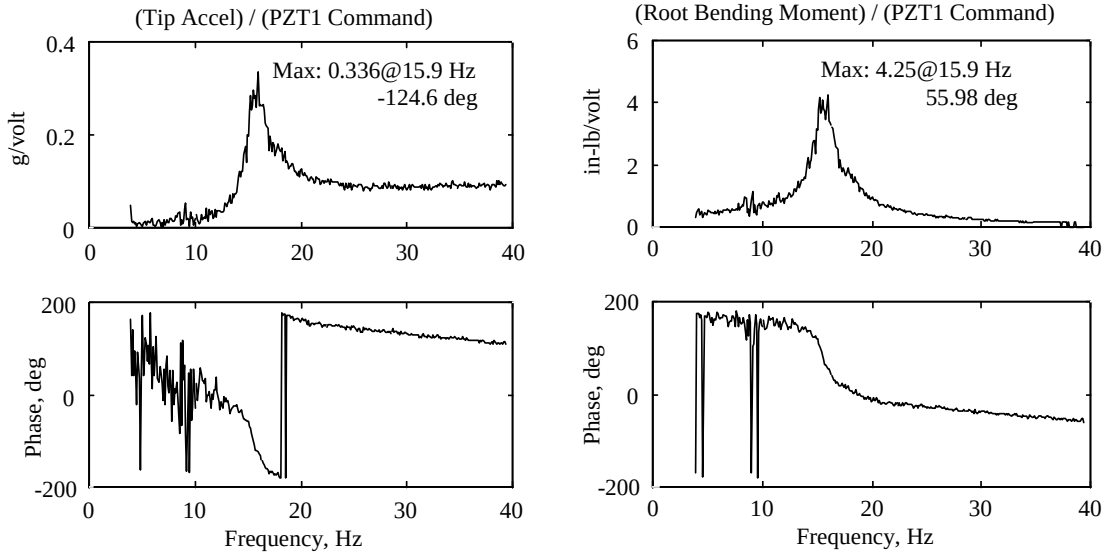

(a) Tip Acceleration/ Piezoelectric Command

(b) Root Bending Moment/ Piezoelectric Command

Figure 11. Open-Loop Frequency Response Functions Between Selected Sensors and Piezoelectric Actuator Command at 14 psf, 12 Degrees AOA

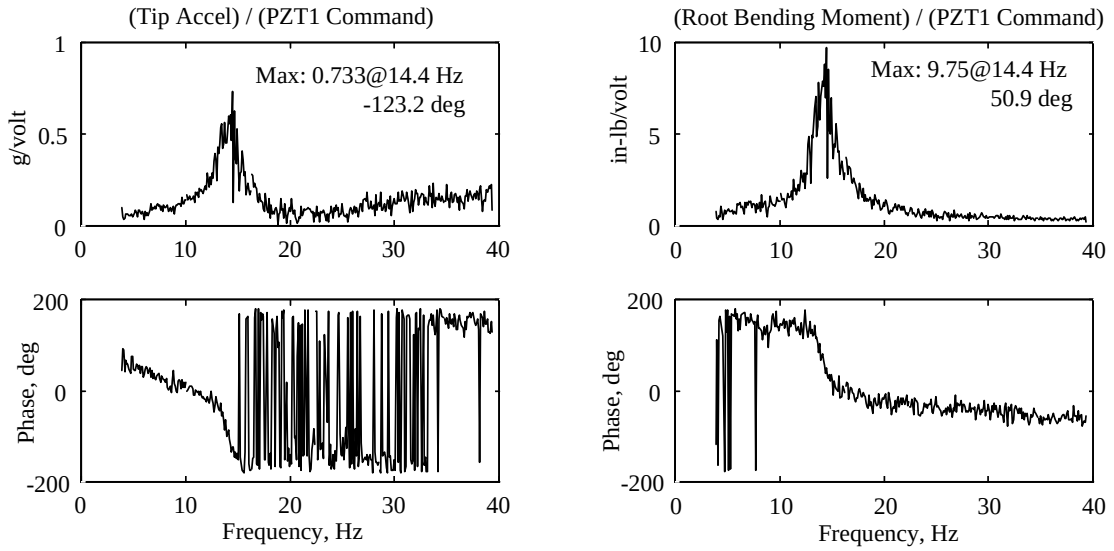

(a) Tip Acceleration/ Piezoelectric Command

(b) Root Bending Moment/ Piezoelectric Command

Figure 12. Open-Loop Frequency Response Functions Between Selected Sensors and Piezoelectric Actuator Command at 14 psf, 24 Degrees AOA

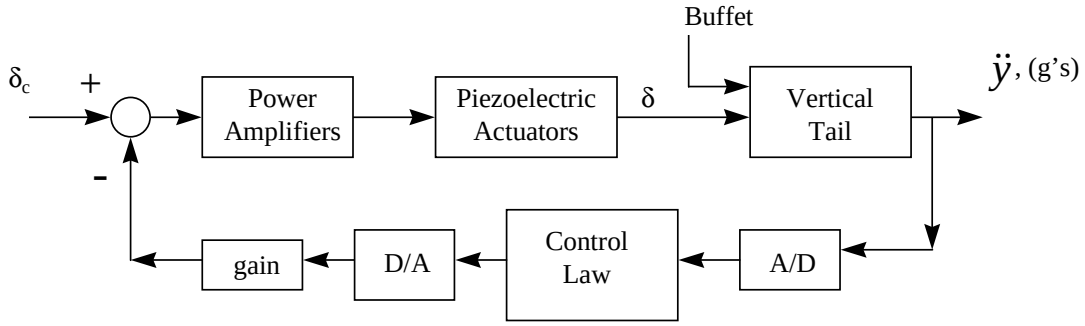

Figure 13. Active Control System

The effectiveness of the seven actuator pairs were studied individually during tail buffeting. The three pairs of actuators at the root of the vertical tail were grouped together to boost actuator authority in the first bending mode. The remaining four pairs of actuators were abandoned because of their lack of authority in the higher tail modes. Open-loop frequency response functions of the 3 pairs of piezoelectric actuators (grouped together as a single actuator) with respect to an accelerometer at the tip near the leading edge and with respect to a root strain gauge (bending moment) are shown in figures 11 and 12 for 12 and 24 degrees angle of attack, respectively. The open-loop frequency response function between actuator command and tip acceleration, shown in figures 11(a) and 12(a), is the input-output relationship of the forward loop of the active control system, shown in figure 13. As shown in figure 13, buffet contributes to the response (output) of the vertical tail (accelerations for this case). For the purpose of computing open-loop transfer functions, the response (output) time histories obtained when the tail was buffeting will contain contributions from the unmeasured buffet (input) and the measured actuator responses (input). Therefore, some uncertainty will exist in the open-loop frequency response functions computed from these time histories because of the unmeasured buffet.

For instance, the amplitude of the peak response in the first bending mode is larger in figure 12 for 24 degrees angle of attack than in figure 11 for 12 degrees angle of attack. Unlike the flow at 12 degrees angle of attack, the flow at 24 degrees angle of attack has components that are contributing to the vibration. The same actuator response signal was used in computing these open-loop frequency response functions. Therefore, the responses measured at 24 degrees angle of attack were not solely due to the commanded actuator but also due to an unmeasured input called buffet.

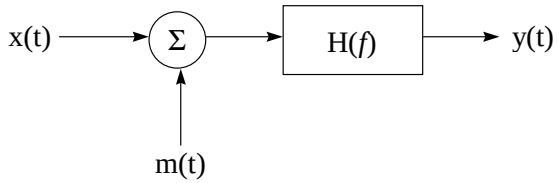

Figure 14. Input Noise Passing Through The System

To better illustrate the effect of an unmeasured input on the system open-loop frequency response function, the forward loop of figure 13, is idealized in figure 14 by two inputs to the vertical tail, one a known command, x(t), and the second an unmeasured noise, m(t). The unmeasured input noise will affect the open-loop frequency response function by overstating the output/input relationship[20]. In terms of physically measurable one-sided (non-negative *f* only) spectral density functions, the input/output relations can be defined as

$$G_{yy}(f) = |H(f)|^2 G_{xx}(f)$$
$$G_{xy}(f) = H(f) G_{xx}(f)$$

Using complex polar notation

$$G_{xy}(f) = |G_{xy}(f)| e^{-j\theta_{xy}(f)}$$
$$H(f) = |H(f)| e^{-j\phi(f)}$$

yields the relations

$$|G_{xy}(f)| = |H(f)| G_{xx}(f)$$
$$\theta_{xy}(f) = \phi(f)$$

Input noise leads to bias errors in the estimation of H(f) by the equation above for $G_{xy}(f)$ because the denominator will no longer be the true input spectrum. The unknown or unmeasured noise m(t) may be correlated with the measured input x(t). For this case, finite Fourier transform of the convolution integral over record length T yields

$$Y(f, T) = H(f) [X(f, T) + M(f, T)]$$

Using the expected value operator for the cross-spectra, given by

$$G_{xy}(f) = \lim_{T\to\infty} \frac{2}{T} E[X_k^*(f, T) Y_k(f, T)] \qquad f > 0$$

the expression for Y(f, T) becomes

$$G_{xy}(f) = H(f) [G_{xx}(f) + G_{xm}(f)]$$

Hence,

$$H(f) = \frac{G_{xy}(f)}{G_{xx}(f) + G_{xm}(f)}$$ = true frequency response function

$$H(f) = \frac{G_{xy}(f)}{G_{xx}(f)}$$ = measured frequency response function

To minimize the uncertainties in the open-loop transfer functions, system identification was performed on time histories acquired at the lower angles of attack. These open-loop transfer functions provide a better estimate of the input/output relationships of the commanded piezoelectric actuators and tail response. However, the effects of the aerodynamics on the vertical tail structural dynamics may not be accurately represented. Therefore, the control law used in alleviating buffeting must be robust.

7.0 Control Law Design For Alleviating Vertical Tail Buffeting

Using the open-loop frequency response functions obtained during the test, control laws were designed using frequency domain compensation methods[21]. These control laws were single-input, single-output control laws that utilized either a tip accelerometer or a root strain gage as the sensor to alleviate the response in the first bending mode. Because of some uncertainty in the measurement of the response created by the buffet at the worst case condition of 34 degrees angle of attack, the control laws were designed based on the open-loop frequency response functions acquired at the lower angles of attack where the buffet, and the uncertainty in the plant, were much less.

The components of the active control system, shown in figure 9, include an analog-to-digital converter (A/D), a digital controller[18] in which the control law is implemented, and a digital-to-analog (D/A) converter. Since there were time delays associated with the digital controller and the actuator, the best approach to control law design was to take advantage of these phase lags. By lagging accelerations by ninety degrees of phase, the commanded motion of the actuator may provide damping to reduce the buffeting of the tail. For the piezoelectric actuators, the digital controller and the distance between the power amplifiers and the actuators were the major contributors to the phase lags. Because the frequency of the first bending mode was higher at the lower angles of attack, as shown in figure 10, the control law was designed to provide a total lag of 90 degrees at the frequency of the first bending mode expected at the higher angles of attack. In designing the control law, it was assumed that the phase relationship between tip accelerations and actuator command would not be a function of angle of attack. The resonance of the piezoelectric actuators was not encountered but was well above 100 Hz. Therefore, significant filtering was added to the control law to reduce its gain beyond 50 Hz so that modes at higher frequencies were not affected. Numerous levels of filtering in the control law were investigated analytically until arriving at the baseline control law, shown in figure 15, which is third order (one zero and four poles). The baseline control law design simply subtracted phase at the first bending mode so that the phase of the actuator lagged tip accelerations by ninety degrees at the frequency of the first bending mode, f_b. For the two phase curves plotted in figure 15, the solid line is the control law as designed and the dashed line is the control law as designed plus the effects of a zero order hold (zoh) to compensate for the D/A converter sampling at 200 Hz. A third order Pade' approximation was used in simulating the zoh during control law design.

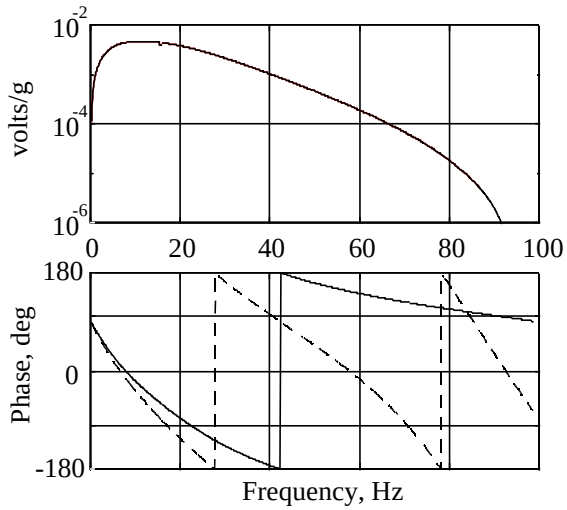

Figure 15. Baseline Control Law Between Tip Acceleration and Piezoelectric Actuator Command With (Dashed) and Without Time Delay

8.0 Open-Loop Controller Performance Evaluation (CPE)

To permit assessing control law performance, near real-time, prior to closing the loop, stability margins were computed for the baseline control law through a process known as controller performance evaluation (CPE) [19]. Using the gain setting, controller performance evaluations (CPE) could be made prior to closing the loop by sending a known command, usually a linear frequency sweep, directly to the actuator and recording the time histories of the command and the

responses. Using MATLAB, the acquired time histories were transformed into an open-loop frequency response function then combined with the baseline control law, and estimates of stability were computed. Because the digital controller and supporting software generated results on-line, assessment of control law performance could be made within minutes. The gain of the control law could be changed prior to commanding the actuator by simply changing the value of gain stored in the digital controller. This allowed a simple and quick assessment of gain on the performance of the control law.

9.0 Active Buffeting Alleviation Results

In figures 16(a) and 16(b), the open-loop and closed-loop tip accelerations and root strains (bending moment), respectively, at 34 degrees angle of attack are overlayed on the same plot to illustrate the buffeting alleviation, out to 50 Hz, created by actively controlling the piezoelectric actuators. The response of the tail in its first bending mode has been decreased with the aid of active piezoelectric actuators, as seen in figure 16. The peak value of the PSD of the root bending moment at the frequency of the first bending mode has been reduced by approximately 60% while the RMS value of the total signal has been reduced by approximately 19%.

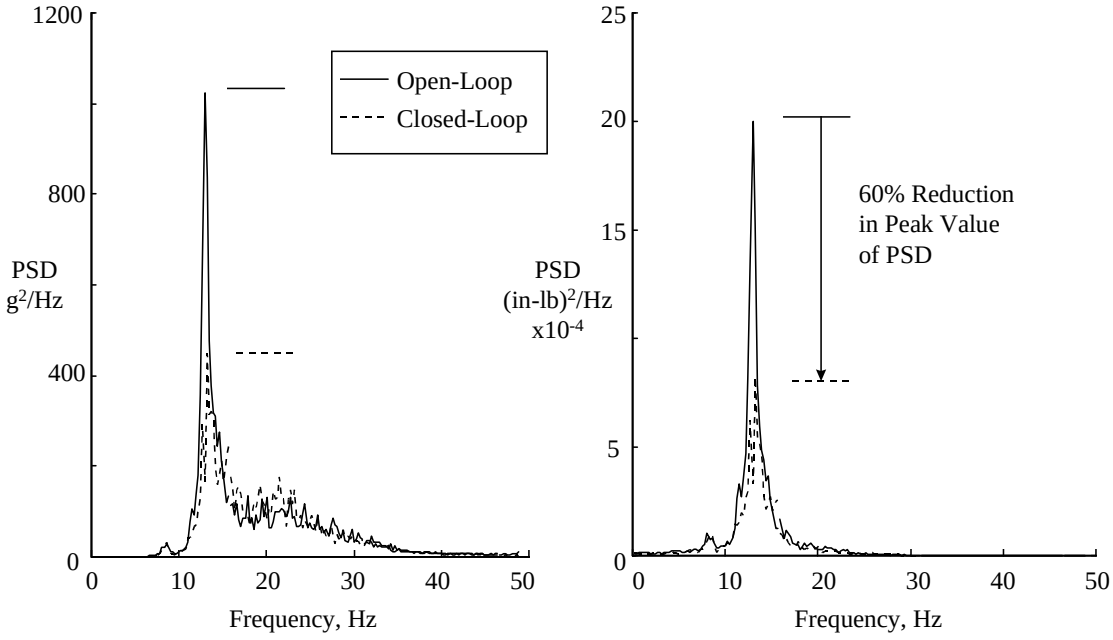

(a) Tip Acceleration (b) Root Bending Moment

Figure 16. Comparison of Selected Responses for Open-Loop (Dotted Line) and Closed-Loop (Solid Line) Piezoelectric Actuators, Test Data Acquired at 14 psf, 34 Degrees AOA

The actively controlled piezoelectric actuators provided damping to the tail for other angles of attack, as summarized in figure 17. The PSD of the root strain (bending moment) was reduced by as much as 60% for certain angles of attack, using a constant gain well below the actuators' physical limits. At the gain setting used for the piezoelectric actuators, 2.4 volts (RMS) of the 10 volts available were used to alleviate the vertical tail buffeting at 34 degrees angle of attack.

On a percentage basis, the buffeting alleviation of both actuators is less at 37 degrees AOA than at 34 degrees AOA. The effectiveness of the actively controlled actuators to add damping appears to be diminishing as angle of attack is increased above 34 degrees. Since the magnitude of the feedback signal at 37 degrees will be similar to the magnitude around 33 degrees angle of attack, the buffeting alleviation result at 37 degrees was expected to be similar to the results around 33 degrees. However, since the force output of the piezoelectric actuators is independent of the aerodynamics, the effectiveness of the piezoelectric actuators should be the same at 33 and 37 degrees angle of attack. Shown in table 1, the aerodynamic damping at 37 degrees angle of attack is higher than the aerodynamic damping around 33 degrees. While the damping due to the feedback signal through the control law would be approximately the same at 33 and 37 degrees, the total damping, without feedback on, has increased at 37 degrees angle of attack. Thus, the percentage of the total damping

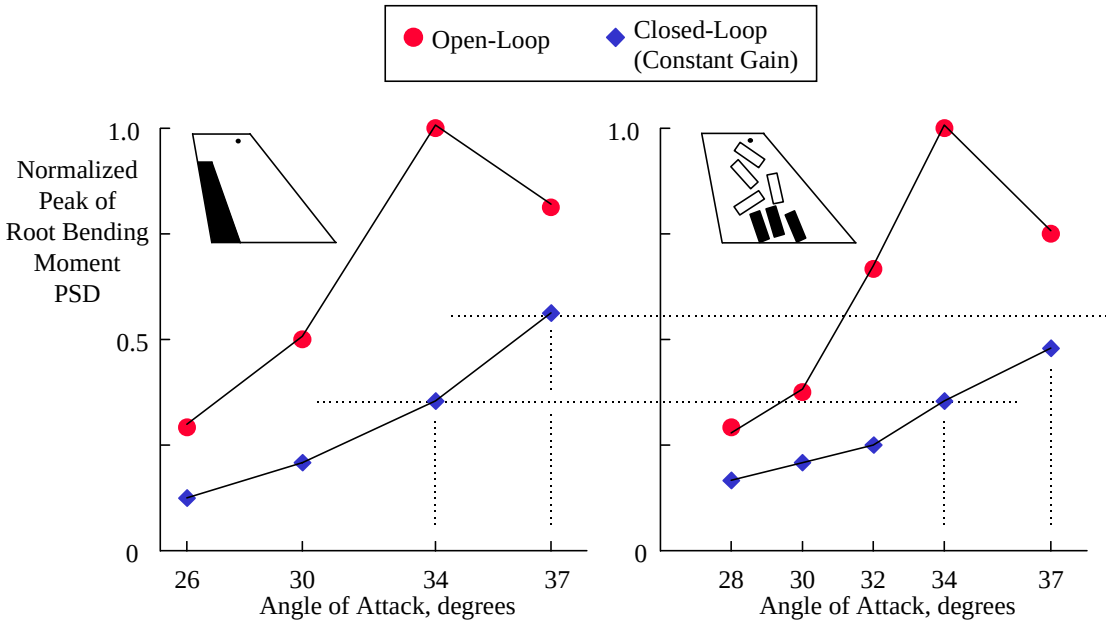

(a) Rudder Results (b) Piezoelectric Actuator Results

Figure 17. Comparisons of the Peak Values of the PSD of the Root Bending Moment at the Frequency of the First Bending Mode for Open-Loop and Closed-Loop Conditions, At Various Angles of Attack, 14 psf

added by the actively-controlled piezoelectric actuators has diminished at 37 degrees compared to 33 degrees angle of attack. In addition, it is interesting to note that the trend of the closed-loop rudder results does differ slightly from the trend of the closed-loop piezoelectric actuator results. This difference may indicate a reduction in aerodynamic effectiveness (force output) of the rudder at 37 degrees compared to 34 degrees angle of attack.

For the baseline control law, stability calculations were performed at numerous angles of attack prior to turning feedback on (closing the loop). The results of the stability calculations were plotted in a Nyquist format, as shown in figure 18, for 20 and 32 degrees angle of attack. For both angles of attack shown in figure 18, the Nyquist curve remains inside the unit circle, indicating that phase margins (negative and positive) are infinite. In figure 19, the stability gain margins (GM), whose values are summarized for the angle of attack range tested, illustrate that the baseline control law at a constant gain setting will not cause any instabilities. Although the gain margin decreases as angle of attack is increased, the gain margin remains greater than zero which indicates stability of the system over the frequency range plotted which is 0 to 20 Hz.

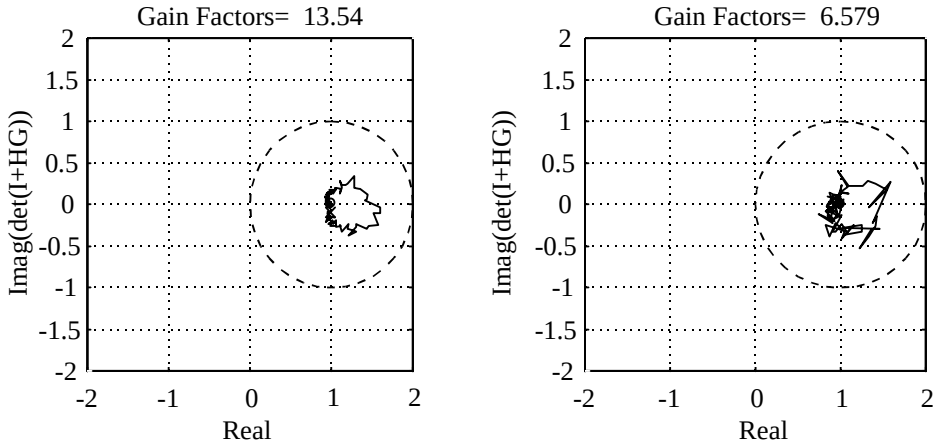

(a) 20 Degrees AOA (b) 32 Degrees AOA

Figure 18. Expected Performance of the Baseline Control Law For 2 Angles of Attack, 14 psf

The effect of the unmeasured buffet (input) on the frequency response function may be the source of the decrease in GM with increased angle of attack. The magnitude of the feedback signal is increasing with increased angle of attack up to 34 degrees where the magnitude of the command is at its maximum. Therefore, based on the stability results, setting the gain of the control law so that amplifier and piezoelectric actuator performance are not exhausted at the worst case (angle of attack) condition does not exclude the alleviation of buffeting at other angles of attack, as seen in figure 19. Based on the results in figures 17 through 19, it is anticipated that further improvement in the closed-loop response may be achieved by simply adjusting the gain in the control law to higher (still stable) values, thereby improving upon the percentage of total damping added to the system through the use of active controls.

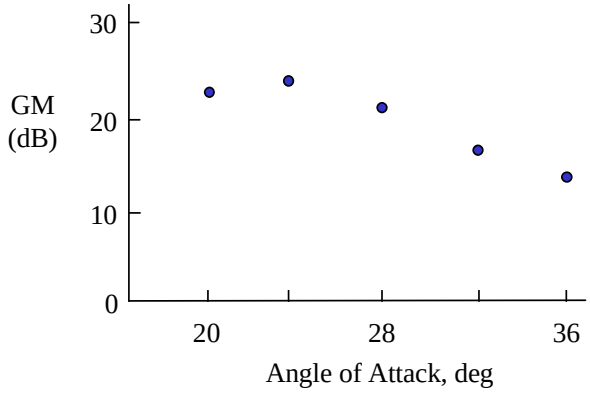

Figure 19. Gain Margins of the Baseline Control Law at Constant Gain, Five Angles of Attack, 14 psf

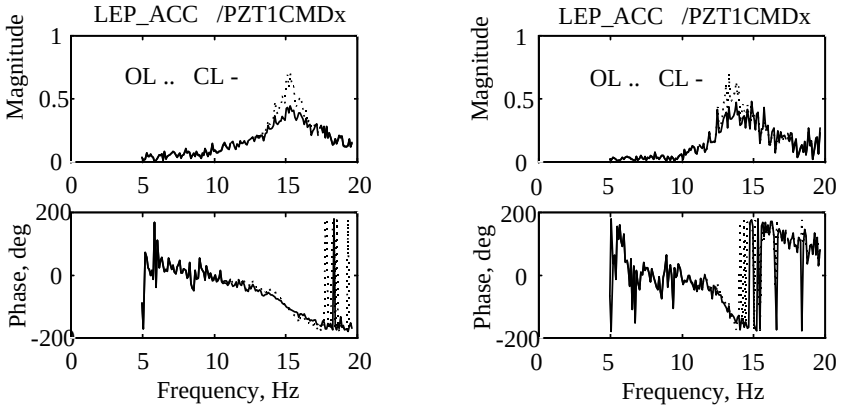

(a) 20 Degrees AOA (b) 32 Degrees AOA

Figure 20. Comparison of Open-Loop and Expected Closed-Loop Frequency Response Functions For 5 Angles of Attack, 14 psf

In addition to stability, estimates of the closed-loop plant were computed prior to closing the loop. As seen in figure 20 for 20 and 32 degrees angle of attack, the peak magnitude of the closed-loop transfer function at each angle of attack is less than the peak magnitude of the respective open-loop transfer function. These reduction in the peak magnitude indicate that damping was added to the system when using the baseline control law.

10.0 Conclusions and Future Plans

During buffeting, the dynamics of the vertical tail are a function of angle of attack, as evident in the shift of the frequency of the first bending mode with angle of attack. When considering the vertical tail as a single degree-of-freedom system, estimates of the aerodynamic damping showed that aerodynamic damping was increasing with increases in angle of attack which means that the total damping (structural plus aerodynamic) without feedback on was increasing as well. Despite

these changes in the structural dynamics of the vertical tail with angle of attack, a single-input-single-output control law was employed successfully at constant gain throughout the entire angle of attack range without requiring adaptations accomplished by scheduling the parameters of the control law.

During the wind-tunnel tests of the ACROBAT program's 1/6-scale F-18 model in the Transonic Dynamics Tunnel, reductions up to 60% in the peak value of the PSD of the root bending moment at the frequency of the first bending mode were observed when using actively controlled piezoelectric actuators or rudder at gains well below their physical limits. For the piezoelectric actuators, only 2.4 volts (RMS) were used of the 10 volts available to obtain the large reductions in root bending moment stated above.

The effectiveness of the control law to alleviate buffeting appeared to drop as angle of attack was increased. At 37 degrees angle of attack, the magnitude of the feedback signal was relatively the same as the magnitude around 33 degrees which means that the magnitude of the damping provided by the controlled actuator was approximately the same at 33 and 37 degrees. Therefore, the percentage of total damping added by feedback control was less at 37 degrees than at 33 degrees angle of attack. By comparison, the rudder provided less buffeting alleviation at 37 degrees angle of attack than did the piezoelectric actuators. The variation in force output of the rudder with angle of attack may have contributed to the reduced buffeting alleviation of the starboard vertical tail at 37 degrees angle of attack.

The stability margins of the system indicated that the gain of the control law may be increased by a factor of four without driving the first bending mode of the vertical tail unstable. Therefore, significant improvements can be achieved simply by increasing the gain of the baseline control law. However, it is anticipated that significant improvements in buffeting alleviation performance over the entire range of angle of attack may be achieved by using adaptive control methods that adjust the parameters of the control law based on angle of attack.

This wind-tunnel investigation was the first demonstration of active vertical tail buffeting alleviation using a rudder and piezoelectric actuators on an F-18 model. Although analyses of such systems have been performed coincidentally using approximations of the unsteady aerodynamics, dependencies on approximations were not necessary during this wind-tunnel investigation since the aerodynamics associated with F-18 aircraft configuration at high angles of attack were represented at wind-tunnel conditions determined using Strouhal scaling.

Based on the success of the ACROBAT program, NASA LaRC has been invited to participate in similar active buffeting alleviation programs hosted by the United States Air Force and McDonnell-Douglas. Through a USAF contract and under the auspices of The Technical Cooperative Program (TTCP), a ground test of a buffet loads alleviation system that uses piezoelectric actuators will be conducted on an F-18 aircraft in late 1997. Separately, McDonnell-Douglas is pursuing wind-tunnel testing of a buffeting alleviation system that uses a neural network to command the rudder based on feedback signals from a strain gauge located at the root of the vertical tail. To assist in this effort, LaRC has invited MDC to participate in wind-tunnel tests in 1998-9 of a follow-on program of ACROBAT called SIDEKIC (Scaling Influences Derived from Experimentally-Known Impacts of Controls on buffet-affected tails). One objective of the SIDEKIC program is to test scaled-replicas of the vertical tails used in the ground test at AMRL (Aeronautical and Maritime Research Laboratory) for the purpose of building a database for deriving scaling laws between model- and full-scale applications of piezoelectric actuators. A second objective of the SIDEKIC program is to perform wind-tunnel tests in support of a proposed flight demonstration of buffet loads alleviation systems beginning in 1999.

11.0 References

1 Zimmerman, N. H., and Ferman, M. A., "Prediction of Tail Buffet Loads for Design Application," Vols. I and II, Rept. No. NADC-88043-60, July 1987.

2 Lee, B. H. K., Brown, D., Zgela, M., and Poirel, D., "Wind Tunnel Investigation and Flight Tests of Tail Buffet on the CF-18 Aircraft", in Aircraft Dynamic Loads Due to Flow Separation, AGARD-CP-483, NATO Advisory Group for Aerospace Research and Development, Sorrento, Italy, April 1990.

3 Pettit, C. L., Brown, D. L., and Pendleton, E., "Wind Tunnel Tests of Full-Scale F/A-18 Twin Tail Buffet: A Summary of Pressure and Response Measurements," AIAA-94-3476, proceedings of the AIAA Atmospheric Flight Mechanics Conference, Scottsdale, AZ, August 1994.

4 White, E. V., “An Active Smart Material System for Buffet Load Alleviation: Functional Requirements Update and Maintenance Information,” presented at the Active Buffet Suppression: Phase II Program Preliminary Design Review Meeting at Active Controls eXperts (ACX), August 4, 1995.
5 Lee, B. H. K. and Tang, F. C., “Unsteady Pressure and Load Measurements on an F/A-18 Vertical Fin at High-Angle-Of-Attack,” AIAA-92-2675-CP, pp. 588-599.
6 Brown, D., Lee, B. H. K., and Tang, F. C., “Some Characteristics and Effects of the F/A-18 LEX Vortices,” Vortex Flow Aerodynamics, AGARD Conference Proceedings 494, Scheveningen, The Netherlands, 1-4 October 1990.
7 Lee, B. H. K. and Tang, F. C., “Buffet Load Measurements on an F/A-18 Vertical Fin at High-Angle-of-Attack,” AIAA 92-2127-CP, AIAA Dynamics Specialist Conference, Dallas, TX, April 16-17, 1992.
8 Pettit, C. L., Banford, M., Brown, D., and Pendleton, E., “Pressure Measurements on an F/A-18 Twin Vertical Tail in Buffeting Flow,” Vols 1-4, United States Air Force, Wright Lab., TM-94-3039, Wright Patterson AFB, OH, August 1994.
9 Meyn, Larry A., and James, Kevin D., "Full-Scale Wind Tunnel Studies of F/A-18 Tail Buffet", AIAA 93-3519, AIAA Applied Aerodynamics Conference, August 9-11, 1993, Monterey, CA.
10 Pettit, C. L., Brown, D. L., Banford, M. P., and Pendleton, E., “Full-Scale Wind-Tunnel Pressure Measurements on an F/A-18 Tail During Buffet,” Journal of Aircraft, Vol. 33, No. 6, Nov.-Dec. 1996, pp. 1148-1156.
11 Meyn, L. A., James, K. D., and Geenen, R. J., “Correlation of F/A-18 Tail Buffet Results,” High-Alpha Projects & Technology Conference, NASA Dryden Flight Research Center, July 12-14, 1994.
12 Meyn, L. A. and James, K. D., “Full-Scale Wind-Tunnel Studies of F/A-18 Tail Buffet,” Journal of Aircraft, Vol. 33, No. 3, May-June 1996.
13 Moses, R. W. and Pendleton, E., “A Comparison of Pressure Measurements Between a Full-Scale and a 1/6-Scale F/A-18 Twin Tail During Buffet,” presented at the 83rd Meeting of the Structures And Materials Panel (SMP) of the Advisory Group for Aerospace Research and Development (AGARD), Florence, Italy, September 2-6, 1996.
14 Ashley, H., Rock, S. M., Digumarthi, R., Chaney, K., and Eggers, A. J. Jr., “Active Control For Fin Buffet Alleviation,” WL-TR-93-3099, January 1994.
15 Lazarus, K. B., Saarmaa, Erik, and Agnes, G. S., “An Active Smart Material System for Buffet Load Alleviation,” SPIE Proceedings Vol. 2447, 1995, pp. 179-192.
16 Hauch, R. M., Jacobs, J. H., Dima, C., and Ravindra, K., “Reduction of Vertical Tail Buffet Response Using Active Control,” Journal of Aircraft, Vol. 33, No. 3, May-June 1996.
17 Moses, R. W., “Vertical Tail Buffeting Alleviation Using Piezoelectric Actuators and Rudder,” High-Angle-of-Attack Technology Conference, September 17-19, 1996, NASA Langley Research Center.
18 Hoadley, S. T. and McGraw, S. M., “Multiple-Function Digital Controller System for Active Flexible Wing Wind-Tunnel Model,” Journal of Aircraft, Vol. 32, No. 1, January-February 1995, pp. 32-38.
19 Wieseman, C. D., Hoadley, S. T., and McGraw, S. M., “On-line Analysis Capabilities Developed to Support the Active Flexible Wing Wind-Tunnel Tests,” Journal of Aircraft, Vol. 32, No. 1, January-February 1995, pp. 39-44.
20 Bendat, J. S. and Piersol, A. G., Engineering Applications of Correlation and Spectral Analysis, Second Edition, John Wiley & Sons, Inc., 1993.
21 Franklin, G. F., Powell, J. D., and Emami-Naeini, A., Feedback Control of Dynamic Systems, Addison-Wesley Publishing Co., Reading MA, 1986.